http://dx.doi.org/10.5012/bkcs.2012.33.2.443

Electrochemical and Fluorescent Properties of Ferrocenyl Chalcones Containing 1-Naphthalenyl Group: X-ray Crystal Structure of Fc-C(O)CH=CH-(1-Naph)

Wooyoung Suh, Hyokyung Jeon, Ji-Yeon Lee, Chae-Mi Lim, Su-Kyung Lee, and Dong-Youn Noh*

*Department of Chemistry, Seoul Women's University, Seoul 139-774, Korea. *E-mail: dynoh@swu.ac.kr*
Received November 17, 2011, Accepted November 29, 2011

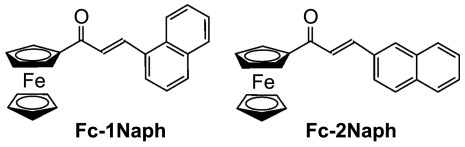
Ferrocenyl chalcones (Fc-C(O)CH=CH-Ar: **Fc-Ar**) with mono- and di-1-naphthalenyl moieties (**Fc-1Naph** and **Fc-d1Naph**) were prepared and spectroscopically characterized. The enone bridge was in the s-*cis* conformation and the π-electrons on the C=C bond were further delocalized on the bridge. The naphthalenyl moiety deviates greatly from the enone-Cp plane by 26.9(1)°. Cyclic voltammetry measurements for **Fc-1Naph** exhibit one reversible cycle for the redox of the ferrocenyl moiety at a lower potential, and one irreversible oxidation peak at the higher potential region. For **Fc-d1Naph**, the cyclic voltammogram is more featureless. Fluorescence properties for both compounds are active in polar solvents with λ_{em} = 500 nm (EtOH) and λ_{em} = 512 nm (MeOH) for **Fc-1Naph** and λ_{em} = 496 nm (EtOH) and λ_{em} = 508 nm (MeOH) for **Fc-d1Naph**. The intensity of **Fc-d1Naph** is more than twice than that of **Fc-1Naph**. The fluorescence properties for both compounds are inactive in the less polar solvents such as CH_3CN, CH_2Cl_2 and $CHCl_3$.

Key Words : Ferrocenyl chalcone, Naphthalene, Electrochemistry, Fluorescence, X-ray crystal structure

Introduction

Ferrocenyl chalcone is a member of chalcone family, in which the ferrocenyl moiety and an aromatic unit, such as a phenyl derivative, are connected by an enone bridge, -C(O)CH=CH-. This system exhibits very versatile biological activities, such as antitumor,[1] antimalarial,[2] antiplasmodial,[3] and nematocidal[4] activities. On the other hand, it also has a broad range of applications in non-linear optical (NLO) materials,[5] organic light emitting diodes (OLED),[6] electrochemical[7] or fluorescent[8] chemosensors, *etc*.

Recently, we intensively investigated the X-ray crystal structures, electrochemical properties, and fluorescence properties of ferrocenyl chalcones linked to several kinds of polycyclic aromatic hydrocarbons (PAH), such as 2-naphthalene,[9] 2-anthracene,[10] 9-anthracene,[11] *N*-ethyl carbazole,[12] and 1-pyrene,[13,14] with mono- or di-derivatizations. Among those, the 2-naphthalene derivative **Fc-2Naph** (Scheme 1) was revealed to be non-fluorescent in solution and in its solid state, even though 2-naphthaldehyde, the precursor to **Fc-2Naph**, is fluorescent (λ_{ex} = 355 nm and λ_{em} = 415 nm) in methanol (5.0×10^{-4} M). The fluorescence of naphthalene was supposed to be quenched by the ferrocenyl moiety, because ferrocene is known to be an effective quencher of excited states.[9] But the ferrocenyl moiety does not always act as a quencher: the ferrocenyl chalcones with mono-1-pyrene,[13] di-1-pyrene,[14] 2-anthracene,[9] and *N*-ethyl carbazole[12] are fluorescent. It is more interesting that the 2-anthracene derivative is fluorescent while the 9-anthracene derivative is not. This implies that the derivatization position on PAH, which in turn determines the structural and electronic characteristics of the compounds, can be one of the critical points for determining the fluorescence of the compounds.

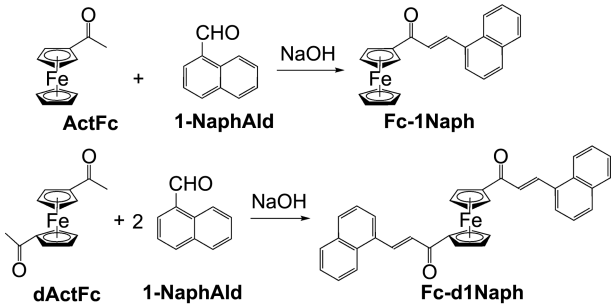


Scheme 1. Structures of **Fc-1Naph** and **Fc-2Naph**.

Along these lines, in order to study on the fluorescence properties of the naphthalenyl derivative of ferrocenyl chalcone, we prepared new ferrocenyl chalcones linked to one (**Fc-1Naph**) and two 1-naphthalene units (**Fc-d1Naph**). Their electrochemical and fluorescent properties, together with the X-ray crystal structure of **Fc-1Naph**, were investigated and explained in comparison with those of **Fc-2Naph**.

Experimental

First grade organic solvents were purchased and used without further purification. Melting points were determined using a Stuart SMP3 (Barloworld Scientific Ltd.). The measurement of the MALDI-TOF (Matrix-Assisted Laser Desorption Ionization-Time of Fight) mass was performed with a Voyager-DE^{TM} STR Biospectrometry Workstation (Applied Biosystems Inc.). The infrared spectra were recorded by the KBr pellet method on a Perkin Elmer Spectrum 100 with a range of 4000-400 cm^{-1}, and the ^{1}H NMR measurements were performed at room temperature using an Avance 500 (Bruker) with the sample dissolved in $CDCl_3$. UV-Vis. spectra were obtained on an HP 8452A diode array spectrophotometer and the fluorescence spectra were measured at room temperature by a Cary Eclipse fluorescence spectrophotometer (Varian) equipped with a Xenon flash lamp. The cyclic voltammetry (CV) and differential pulse voltammetry (DPV) were carried out at room temperature with a CHI 620A Electrochemical Analyzer (CHI



Scheme 2. Synthesis of **Fc-1Naph** and **Fc-d1Naph**.

Instrument Inc.) in 3.0 mL CH_3CN solution containing a 0.5 mM of the sample, using 0.1 M *n*-$Bu_4N{\cdot}BF_4$ as a supporting electrolyte, Ag/AgCl as a reference electrode, a Pt button working electrode, a Pt wire as a counter electrode, and with a scan rate of 100 mV s^{-1}. All redox potentials were referenced against the Fc^+/Fc redox couple ($E_{1/2}$ = 0. 474 V).

Preparation of Fc-1Naph. A solution of acetylferrocene (**ActFc**: 1.0 mmol, 0.228 g), and 1-naphthaldehyde (**1NaphAld**: 1.0 mmol, 0.135 mL) in ethanol (20 mL) was stirred overnight at room temperature in the presence of NaOH (5.0 mmol, 0.198 g). (Scheme 2) The red solution was evaporated and then the product was extracted with CH_2Cl_2 and then dried with $MgSO_4$. After filtration, the red solution was evaporated and separated by column chromatography. The dark red bands were separated by toluene:ethyl acetate (from 2.5:1 to 4:1) and crystallized from CH_2Cl_2/*n*-hexane. Yield 54% (196 mg). mp 139-141 °C. MALDI-TOF-MS (*m/z*, %) 366.0250 (M^+, 100). FT-IR (KBr, cm^{-1}) 3109, 3084, 3060 (Ar C-H), 1642 (C=O), 1593, 1582, 1571, 1453 (C=C), 1378, 1346, 1308, 1260, 1233, 1076 (Ar C=C), 1028, 1005, 988 (Ar C-H ip def), 822, 795, 777 (Ar C-H oop def), 531, 498, 486 (Fe-ring vib). UV (MeOH, nm) 256 m, 350 m, 506 w. ^{1}H NMR (500 MHz, $CDCl_3$, ppm) δ 8.63 (1H, CH=C*H*-CO, d, *J* = 15.4 Hz), 8.32 (1H, CH, d, *J* = 8.51 Hz), 7.91 (3H, CH, m), 7.60 (1H, CH, t, *J* = 14.0 Hz), 7.53 (2H, CH, m), 7.22 (1H, C*H*=CH-CO, d, *J* = 15.4 Hz), 4.96 (2H, C_p, t, *J* = 3.75 Hz), 4.62 (2H, C_p, t, *J* = 3.85 Hz), 4.25 (5H, C_p, s).

Preparation of Fc-d1Naph. Fc-d1Naph was prepared following the same method used for **Fc-1Naph**, using 1,1'-diacetylferrocene (1.0 mmol, 0.270 g), 1-naphthaldehyde (2.0 mmol, 0.271 mL), and NaOH (5.0 mmol, 0.198 g) in ethanol (20 mL). The orange solution was worked-up with the same manner and purified by column chromatography using toluene:ethyl acetate = 2.5:1. The product was crystallized from CH_2Cl_2/*n*-hexane. Yield 29% (153 mg). mp 180-182 °C. MALDI-TOF-MS (*m/z*, %) 546.1537 (M^+, 100). FT-IR (KBr, cm^{-1}) 3119, 3090, 3059 (Ar C-H), 1647 (C=O), 1595, 1584, 1571, 1455 (C=C), 1380, 1348, 1259, 1235, 1098, 1081 (Ar C=C), 1035, 1006, 981 (Ar C-H ip def), 829, 816, 799, 777 (Ar C-H oop def), 531, 486, 456 (Fe-ring vib). UV (MeOH, nm) 260 m, 354 m. ^{1}H NMR (500 MHz, $CDCl_3$, ppm) δ 8.61 (2H, CH=C*H*-CO, d, *J* = 15.3 Hz), 8.21 (2H, CH, qr, *J* = 9.61 Hz), 7.86 (6H, CH, m), 7.52 (4H, CH, m, *J* = 9.55 Hz), 7.37 (2H, CH, t, *J* = 7.69 Hz), 7.16 (2H, C*H*=CH-CO, d, *J* = 15.3 Hz), 5.01 (4H, C_p, t, *J* = 3.79 Hz), 4.65 (4H, C_p, t, *J* = 3.77 Hz).

Table 1. Crystal data and structure refinement parameters for **Fc-1Naph**

Empirical formula	$C_{23}H_{18}FeO$
Formula weight	366.22
Crystal system	orthorhombic
Space group	$Pna2_1$ (No. 33)
a (Å)	28.3932(18)
b (Å)	5.7738(4)
c (Å)	10.3205(7)
Volume (Å^3)	1691.9(2)
Z	4
Absorption coefficient (mm^{-1})	0.898
F(000)	760
Crystal size (mm^3)	0.26 × 0.18 × 0.15
Theta range for data collection	1.43 to 28.28°
Index ranges	$-37 \le h \le 37$, $-7 \le k \le 7$, $-11 \le l \le 13$
Reflections collected	11991
Independent reflections	3868 [R(int) = 0.0945]
Completeness to theta = 28.29°	100.0%
Absorption correction	None
Refinement method	Full-matrix least-squares on F^2
Data / restraints / parameters	3868 / 1 / 226
Goodness-of-fit on F^2	0.965
Final R indices [$I > 2\sigma(I)$]	R1 = 0.0500, wR2 = 0.0957
R indices (all data)	R1 = 0.1095, wR2 = 0.1581
Largest diff. peak and hole	0.690 and −0.782 e.Å^{-3}

X-ray Structure Analysis of Fc-1Naph. The brown plate single crystals of **Fc-1Naph** that were suitable for X-ray structure analysis were grown by the slow-diffusion method in a CH_2Cl_2/*n*-hexane solvent pair. The X-ray crystallographic data for this single crystal was collected on a SMART APEX CCD SYSTEM (Bruker) equipped with a graphite-monochromated Mo K_α (λ = 0.71073 Å) radiation source and a nitrogen cold stream (200(2) K). The structure was solved

Table 2. Selected bond lengths [Å] and angles [°] for **Fc-1Naph**

bond length			
C-C(in Fc)	1.399(10)-1.441(8)	C-C(in Naph)	1.339(12)-1.436(8)
C1-C11	1.472(8)	C11-O1	1.229(7)
C11-C12	1.476(8)	C12-C13	1.340(8)
C13-C14	1.457(9)		
bond angle			
O1-C11-C1	120.2(5)	O1-C11-C12	120.8(6)
C1-C11-C12	119.0(5)	C13-C12-C11	121.7(6)
C12-C13-C14	128.0(6)		
torsion angle			
C13-C12-C11-O1	3.6(5)	C11-C12-C13-C14	-174.6(0)
C12-C11-C1-C2	167.5(1)	C12-C13-C14-C15	153.1(1)

by the direct method and refined by a full-matrix least-squares analysis using anisotropic thermal parameters for non-hydrogen atoms with the SHELXTL program.[15] All of the non-hydrogen atoms were refined anisotropically, and hydrogen atoms were added to their geometrically ideal positions. The crystallographic data and the details of the data collection are listed in Table 1, and the selected bond distances and angles are summarized in Table 2.

Results and Discussion

Synthesis and Characterization. Fc-1Naph was obtained with a 54% yield by refluxing the reactants with an excess amount of catalytic NaOH. **Fc-d1Naph** was also obtained by the same method but in a lower yield (29%). These compounds were also synthesized by the solvent-free grinding method with almost the same yields, and they are spectroscopically identical with those obtained by the refluxing method. Strong ν(C=O) frequencies of **Fc-1Naph** and **Fc-d1Naph** were observed at 1642 and 1647 cm^{-1}, respectively. They are comparable to those of the reactants (**ActFc** and **dActFc**) that are commonly observed at 1663 cm^{-1}. Moreover, the ν(C=O) frequencies of **Fc-2Naph** (1650 cm^{-1}),[9] **Fc-9Anth** (1650 cm^{-1}),[11] **Fc-EtCbz** (1642 cm^{-1}),[12] **Fc-1Pyr** (1645 cm^{-1}),[13] and **Fc-d1Pyr** (1648 cm^{-1}),[14] where the carbonyl moiety is directly linked to the ferrocenyl group, are very close to those of the **Fc-1Naph** and **Fc-d1Naph** compounds. On the contrary, **9Anth-Fc** (1607 cm^{-1})[11] and **1Pyr-Fc** (1611 cm^{-1})[13] where the carbonyl moiety is directly linked to the PAH group (**PAH-Fc**), show a ν(C=O) frequency 30-40 cm^{-1} lower than **Fc-PAH**. Therefore, this ν(C=O) frequency can be a simple index that distinguishes **Fc-PAH** from **PAH-Fc** as well as their reactants.

X-ray Structure Analysis of Fc-1Naph. The X-ray structure analysis of the **Fc-1Naph** single crystal shows that it crystallizes in an orthorhombic system with space group $Pna2_1$ (No 33). The bond length of C12=C13 in **Fc-1Naph** is 1.340(8) Å as shown in Table 2, which is longer than that of **Fc-2Naph** (1.325(5) Å),[9] while the other C-C and C=O bond lengths in the enone moiety are the same in these two isomers within an error range. This indicates that the enone linkage in **Fc-1Naph** is electronically more delocalized than that in **Fc-2Naph**, and this could make the electronic communication between 1-naphthalene and ferrocenyl moieties facile. Therefore, the donor character of the ferrocenyl moiety can affect the emission property of the 1-naphthalene moiety *via* the more delocalized enone linkage in **Fc-1Naph**.

The molecular structure of **Fc-1Naph** (Fig. 1) shows that the C11=O1 and C12=C13 double bonds of the intervening C11-C12 single bond in the enone moiety are in the s-*cis* conformation. As for the **Fc-PAH** compounds where the carbonyl moiety is directly linked to the ferrocenyl group, such as in **Fc-2Naph**,[9] **Fc-9Anth**,[11] **Fc-EtCbz**,[12] and **Fc-d1Pyr**,[14] this type of s-*cis* conformation is usually observed. In comparison, however, the s-*trans* conformation is found in the molecular structures of **2Anth-Fc**[10] and **9Anth-Fc**,[11] in which the carbonyl moiety is directly linked to the anthracenyl group. The molecular structure of **Fc-1Naph** (Fig. 1) and its torsion angles (Table 2) indicate that the enone bridge is almost planar with a torsion angle of 3.6(5)° for ∠C13-C12-C11-O1, as well as the Cp ring (0.6(2)° for ∠C1-C2-C3-C4) and naphthalenyl ring (1.5(1)° for ∠C14-C16-C19-C21). The planar naphthalenyl group, however, significantly deviates from the co-planarity with the plane made by the enone moiety, giving the dihedral angle of about 26.9(1)° for ∠C12-C13-C14-C15. The Cp ring also deviates with the dihedral angle of 12.5(1)° for ∠C12-C11-C1-C2. These deviations of co-planarity may block the quenching ability of the effective ferrocenyl quencher.[16] These structural characteristics are comparable to that of non-fluorescent **Fc-2Naph**, where the enone and naphthalenyl moieties are almost co-planar with a dihedral angle of 4.4(3)°. Combining both factors, the delocalization of the C12=C13 bond in the enone moiety and the deviation of co-planarity among the Cp ring, enone, and naphthalenyl moieties, and assuming that the molecular structure in the solid state is not significantly modified in solution, **Fc-1Naph** is fluorescent in contrast to non-fluorescent **Fc-2Naph**, as will be discussed below.

In the crystal packing mode of **Fc-1Naph** viewed normal to the *ac*-plane (Fig. 2), the two enantiomers are found in a crystal structure. These enantiomers stack along the *b*-axis, therefore, the alternative ferrocenyl and naphthalenyl layers are formed in the *bc*-plane with a long separation between

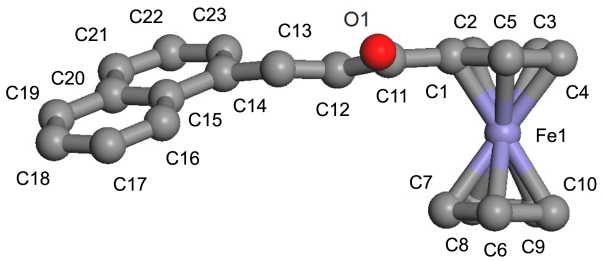


Figure 1. Molecular structure of **Fc-1Naph** with an atomic numbering scheme.

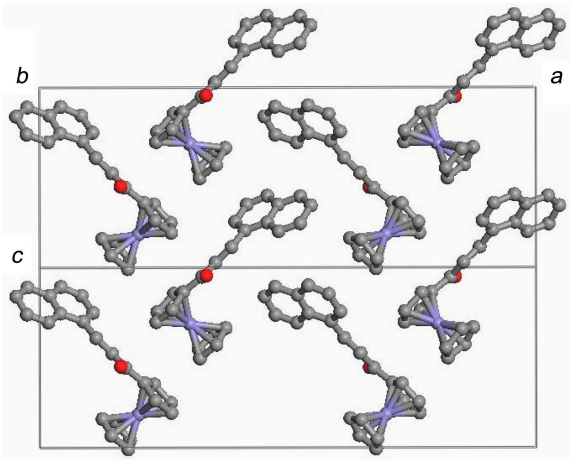


Figure 2. Crystal packing mode of **Fc-1Naph** viewing down to *ac*-plane.

Fe(II) centers (5.7738(4) Å), enough to ignore any electronic interaction.

Electrochemical Properties. The electrochemical properties of **Fc-1Naph** and **Fc-d1Naph** were investigated by cyclic voltammetry (CV) and differential pulse voltammetry (DPV), as shown in Figure 3 and Figure 4, respectively. The parameters are listed in Table 3 and compared with their reactants and **Fc-2Naph**. The CV of **Fc-1Naph** shows one reversible cycle at $E_{1/2}$ = 0.727 V, corresponding to the redox process of the ferrocenyl unit (inset of Fig. 3(a)), and one irreversible anodic peak at E_{pa} = 1.817 V, corresponding to the irreversible oxidation of the naphthalenyl unit. These potentials are very close to those of **Fc-2Naph** ($E_{1/2}$ = 0.719 V and E_{pa} = 1.878 V),[9] as well as that of **ActFc** ($E_{1/2}$ = 0.725 V). However, the half-wave potential ($E_{1/2}$) of the first cycle for **Fc-d1Naph** is more anodic by about 0.2 V than is **Fc-1Naph** because of the greater substitution of the ferrocenyl unit, while the anodic potential (E_{pa}^2) of the naphthalenyl unit is not shifted as much for the three ferrocenyl-naphthalene compounds (1.791-1.878 V) listed in Table 3. The shape of CV of **Fc-d1Naph** is somewhat featureless with a very week reduction peak of the ferrocenyl unit. But the narrow scanning between 0.5 V and 1.3 V (inset of Fig. 4(a)) exhibits a reversible cycle for the ferrocenyl unit. This indicates that the reduction of ferrocenyl unit in **Fc-d1Naph** is significantly influenced by the previous redox history like the redox of naphthalenyl unit, in contrast to **Fc-1Naph**.

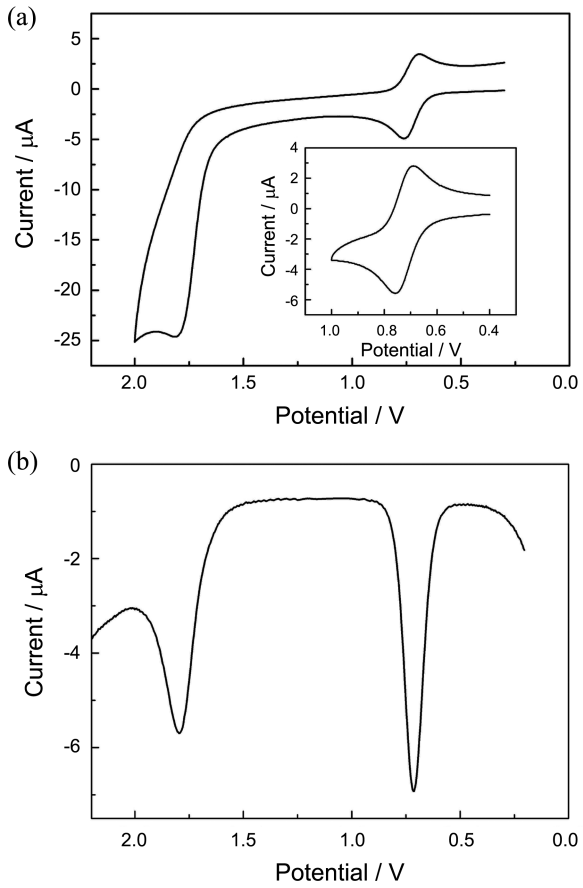


Figure 3. CV (a) and DPV (b) of **Fc-1Naph** with the reversible cycle for the redox process of the ferrocenyl unit shown in the inset of (a).

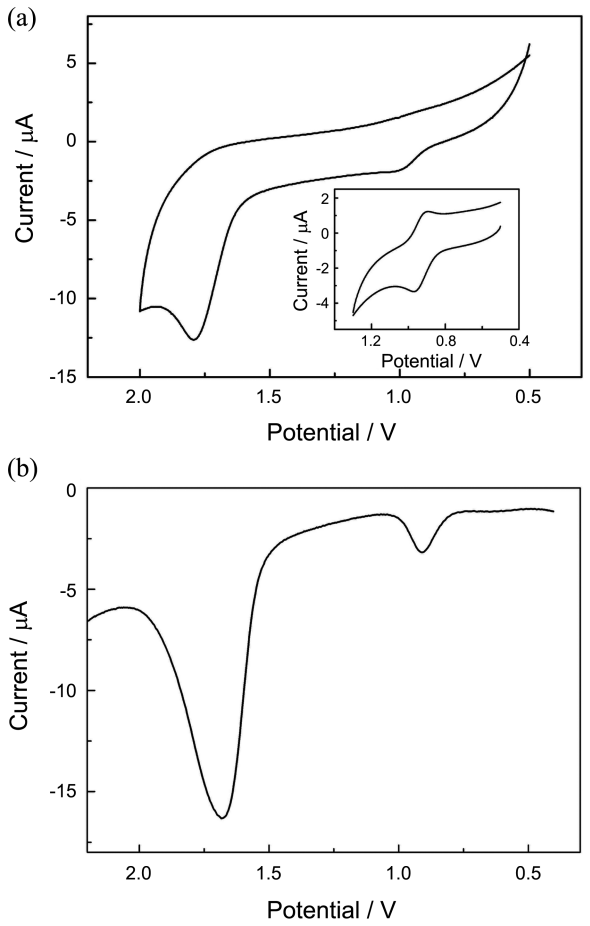


Figure 4. CV (a) and DPV (b) of **Fc-d1Naph** with the reversible cycle for the redox process of the ferrocenyl unit shown in the inset of (a).

Fluorescence Properties. The fluorescence spectra of **Fc-1Naph** and **Fc-d1Naph**, which are dissolved in polar solvents, such as methanol (E_N^T = 0.762 where E_N^T is a normalized empirical parameter of solvent polarity),[17,18] and ethanol (E_N^T = 0.654) with a concentration of 1.5 × 10^{-5} M, are shown in Figure 5 and 6, respectively, coupled with their excitation spectra. Even though both compounds are also

Table 3. Cyclic voltammetry parameters of **Fc-1Naph** and **Fc-d1Naph** compared with their reactants and **Fc-2Naph** (in volts)[a]

Compound	E_{pa}^1	E_{pa}^2	E_{pc}^1	$E_{1/2}$[b]
ActFc	0.761		0.689	0.725
dActFc	0.988		0.913	0.951
1NaphAld		2.054		
Fc-1Naph	0.761	1.817	0.692	0.727
Fc-2Naph[c]	0.755	1.878	0.682	0.719
Fc-d1Naph	0.972	1.791	0.897	0.935

[a]Supporting electrolyte: 0.1 M n-$Bu_4N{\cdot}BF_4$; Working electrode: Pt disk; Counter electrode: Pt wire; Ref. electrode: Ag/AgCl; 0.5 mM samples in CH_3CN; 100 mV s^{-1} scan rate; $E_{1/2}$ = 0.474 V for Fc^+/Fc. [b]$E_{1/2} = (E_{pa}^1 - E_{pc}^1)/2$. [c]ref. 9.

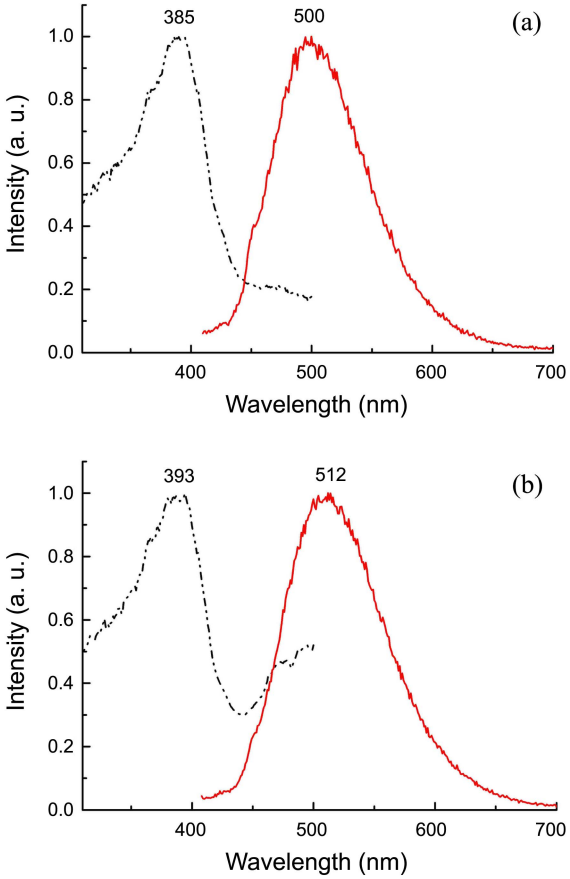


Figure 5. Normalized optical absorption (broken line) and emission (solid line) spectra of **Fc-1Naph** (1.5×10^{-5} M) dissolved in ethanol (a) and methanol (b).

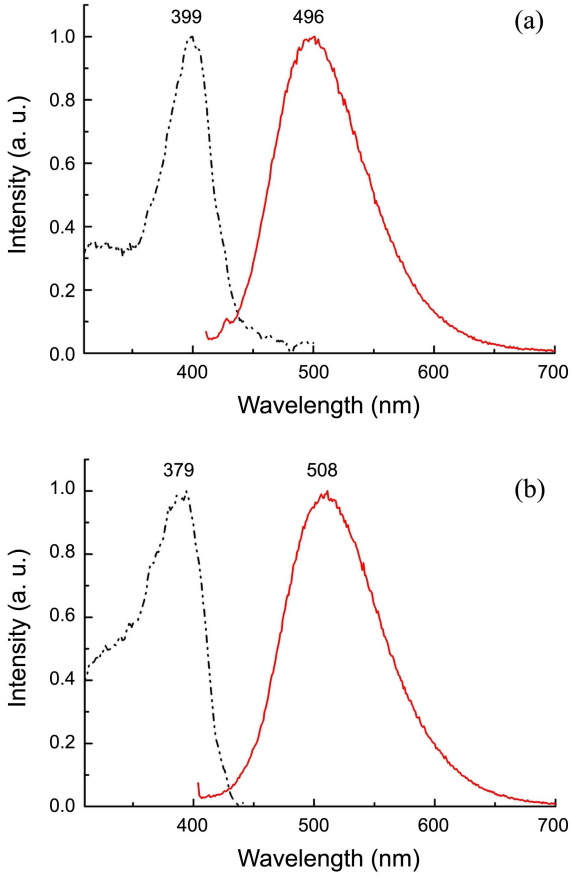


Figure 6. Normalized optical absorption (broken line) and emission (solid line) spectra of **Fc-d1Naph** (1.5×10^{-5} M) dissolved in ethanol (a) and methanol (b).

soluble in less polar solvents, such as CH_3CN ($E_N^T = 0.460$), CH_2Cl_2 ($E_N^T = 0.309$), and $CHCl_3$ ($E_N^T = 0.259$), fluorescence was not observed. An emission peak was observed at 500 nm for **Fc-1Naph** and at 496 nm for **Fc-d1Naph** in ethanol. The bathochromic shift from the emission of the reactant, 1-naphthaldehyde ($\lambda_{ex} = 407$ nm and $\lambda_{em} = 483$ nm in ethanol), is ascribed to the functionality of the ferrocenylenone group linked to the 1-position of naphthalene. This is related to the fact that **Fc-2Naph** is non-fluorescent,[9] while 2-naphthaldehyde is fluorescent ($\lambda_{ex} = 311$ nm and $\lambda_{em} = 425$ nm in 5.0×10^{-4} M ethanol solution).

The emission intensity (I_{em}) and absorptivity (ε_{em}) of the compounds are compared in Table 4. It is noted that the absorptivity of the di-naphthalene compound **Fc-d1Naph** is 4 times more intense than that of the mono-naphthalene **Fc-1Naph** when measured in the same conditions with a concentration of 1.5×10^{-5} M.

In conclusion, ferrocenyl chalcones with one and two 1-naphthalenes (**Fc-1Naph** and **Fc-d1Naph**) were prepared and characterized. These compounds were fluorescent in polar solvents (ethanol and methanol) but non-fluorescent in less polar solvents (CH_3CN, CH_2Cl_2, and $CHCl_3$). These properties are comparative to their isomer, **Fc-2Naph**, which was non-fluorescent in the above solvents. This is likely to stem from the structural differences in which 1-naphthalene and the enone-Cp ring yield a larger dihedral angle (26.9(1)°) in **Fc-1Naph** than that observed in **Fc-2Naph** (4.4(3)°). These differences result in the well-known quencher (ferrocenyl moiety) having less influence on the fluorophore (naphthelenyl moiety), and this consequently results in the fluorescent **Fc-1Naph**.

Table 4. Comparison of the fluorescence intensities (I_{em}) and molar absorptivities (ε_{em}) for the emission peaks of **Fc-1Naph** and **Fc-d1Naph** dissolved in EtOH and MeOH[a]

Solvent	Fc-1Naph			Fc-d1Naph		
	λ_{em} (nm)	I_{em}	ε_{em}[b]	λ_{em} (nm)	I_{em}	ε_{em}[b]
EtOH	500	13.4	8.9×10^5	496	57.9	3.9×10^6
MeOH	512	18.1	1.2×10^6	508	76.4	5.1×10^6

[a]Concentration: 1.5×10^{-5} M. [b]in $M^{-1}cm^{-1}$.

Acknowledgments. This work was supported by a Special Research Grant from Seoul Women's University (2011).

Appendix A. Supplementary Data. CCDC 823245 contains the supplementary crystallographic data for **Fc-1Naph**. This data can be obtained free of charge *via* http://www.ccdc.cam.ac.uk/conts/retrieving.html, or from the Cambridge Crystallographic Data Centre, 12 Union

Road, Cambridge CB2 1EZ, UK; fax: (+44) 1223-336-033; or e-mail: deposit@ccdc.cam.ac.uk.

References

1. Zsoldos-Mady, V.; Csampai, A.; Szabo, R.; Meszaros-Alapi, E.; Pasztor, J.; Hudecz, F.; Sohar, P. *Chem. Med. Chem.* **2006**, *1*, 1119.
2. (a) Wu, X.; Wilairat, P.; Go, M. L.; *Bioorg. Med. Chem. Lett.* **2002**, *12*, 2299. (b) Liu, M.; Wilairat, P.; Go, M. L. *J. Med. Chem.* **2001**, *44*, 4443.
3. Wu, X.; Tiekink, E. R. T.; Kostetski, I.; Kocherginsky, N.; Tan, A. L. C.; Khoo, S. B.; Wilairat, P.; Go, M. L. *Eur. J. Pharm. Sci.* **2006**, *27*, 175.
4. Attar, S.; O'Brien, Z.; Alhaddad, H.; Golden, M. L.; Calderón-Urrea, A. *Bioorg. Med. Chem.* **2011**, *19*, 2055.
5. Kawabe, Y.; Ikeda, H.; Sakai, T.; Kawasaki, K. *J. Mater. Chem.* **1992**, *2*, 1025.
6. Sens, R.; Drexhage, K. H. *J. Lumin.* **1981**, *24-25*, 709.
7. (a) Delavaux-Nicot, B.; Maynadié, J.; Lavabre, D.; Lepetit, C.; Donnadieu, B. *Eur. J. Inorg. Chem.* **2005**, 2493. (b) Delavaux-Nicot, B.; Maynadié, J.; Lavabre, D.; Fery-Forgues, S. *J. Organomet. Chem.* **2007**, *692*, 874.
8. Delavaux-Nicot, B.; Fery-Forgues, S. *Eur. J. Inorg. Chem.* **1999**, 1821.
9. (a) Son, K. I.; Noh, D. Y. *J. Korean Chem. Soc.* **2007**, *51*, 591. (b) CCDC 836352.
10. Lee, S. K.; Lim, C. M.; Lee, J. Y.; Noh, D. Y. *Bull. Korean Chem. Soc.* **2011**, *32*, 321.
11. Jung, Y. J.; Son, K. I.; Oh, Y. E.; Noh, D. Y. *Polyhedron* **2008**, *27*, 861.
12. Son, K. I.; Kang, S. Y.; Noh, D. Y. *Bull. Korean Chem. Soc.* **2009**, *30*, 513.
13. Son, K. I., Ph.D. Thesis, Seoul Women's University, Seoul, 2008.
14. Lee, S. K.; Noh, Y. S.; Son, K. I.; Noh, D. Y. *Inorg. Chem. Commun.* **2010**, *13*, 1343.
15. Sheldrick, G. M. SHELXTL, ver. 5, Bruker AXS, Madison, Wisconsin, 1995.
16. Fery-Forgues, S.; Delavaux-Nicot, B. *J. Photochem. Photobio. A: Chem.* **2000**, *132*, 137.
17. Reichardt, C. *Solvents and Solvent Effects in Organic Chemistry*, 3rd ed.; Wiley: Weinheim, Germany, 2003.
18. Reichardt, C. *Chem. Rev.* **1994**, *94*, 2319.